Revised Version

Single-crystal UV/Vis Optical Absorption Spectra of Almandine-Bearing and Spessartine Garnet: Part II. An Analysis of the Spin-Forbidden Bands of Fe^{2+}, Mn^{2+}, and Fe^{3+}

Michail N. Taran[1], Charles A. Geiger[2,*], Oleksii A. Vyshnevskyi[1] and George R. Rossman[3]

[1] M.P. Semenenko Institute of Geochemistry and Mineralogy and Ore Formation
National Academy of Sciences of Ukraine
Palladin Ave. 34
03142 Kyiv-142, Ukraine

[2] Department Chemistry and Physics of Materials
University of Salzburg
Jakob Haringer Str. 2a
A-5020 Salzburg, Austria

[3] Division of Geological and Planetary Sciences
California Institute of Technology
Pasadena, CA, 91125-2500, USA

[*]Corresponding author
Fax: ++43-662-8044-6289
Tel.: ++43-662-8044-6226
E-mail: ca.geiger@sbg.ac.at

Written using a Macintosh with Word 16.16.3

Date: 01.06.2022

ABSTRACT

The UV/Vis single-crystal absorption spectra of two almandine-bearing and several spessartine garnets were measured and their respective Fe^{2+} and Mn^{2+} spin-forbidden electronic transitions analyzed. Spin-forbidden bands of Fe^{3+} are also considered, because many aluminosilicate garnets contain some Fe^{3+}. The spectra of the almandine-bearing garnets were recorded at room temperature (RT) between about 10000 cm^{-1} and 30000 cm^{-1}. The spectrum of a nearly end-member spessartine (97 mol % $Mn^{2+}_3Al_2Si_3O_{12}$) was measured between about 15000 cm^{-1} and 30000 cm^{-1} at RT and 78 K, the latter for the first time. The 78 K spectrum shows absorption features not observed at RT. Five additional spessartine-rich garnets with different $Mn^{2+}/(Mn^{2+} + Fe^{2+})$ ratios, and two with unusual chemistries, were recorded up to 26000 cm^{-1}. The spectra of the two almandine-bearing garnets agree well with published results and show a number of overlapping $Fe^{2+/3+}$ bands located between about 14000 and 25000 cm^{-1}. The spectra were deconvoluted to gain more insight into the electronic transition behavior. These results, together with an analysis of other measured spectra, reveal several absorption features that were previously unrecognized or misassigned. The spectrum of spessartine shows a number of Mn^{2+} bands and most are clearly spaced from one another. A synthesis of various UV/Vis spectroscopic results is made and assignments for the $Fe^{2+/3+}$ and Mn^{2+} bands are attempted. The intensities of the Mn^{2+} spin-forbidden bands and the ligand $\rightarrow$ metal charge edge observed in the various spessartine spectra are discussed. Spectra of almandine and spessartine have been interpreted using Tanabe-Sugano diagrams that are constructed for cations in octahedral coordination, point symmetry O_h. However, such as analysis does not appear to be fully successful because Fe^{2+} and Mn^{2+} in garnet have triangular dodecahedral coordination with point symmetry D_2. The interpretation of the spectrum of spessartine is especially problematic. An analysis shows that published model calculations of Fe^{2+} electronic transition energies in garnet are not in good agreement with each other and are

59 also not in full agreement with experimental spectra. First principles calculations are needed to
60 better understand the spin-forbidden transitions of Fe^{2+}, Fe^{3+} and Mn^{2+} in garnet.

61 **Key words:** UV/Vis absorption spectroscopy, garnet, almandine, spessartine, spin-forbidden
62 electronic transitions, transition metals, crystal field theory.

63
64
65
66
67
68
69
70
71
72
73
74
75
76
77
78
79
80
81
82
83
84

INTRODUCTION

Almandine and spessartine are commonly occurring aluminosilicate garnets with the ideal end-member crystal-chemical formulas $\{Fe^{2+}_3\}[Al_2](Si_3)O_{12}$ and $\{Mn^{2+}_3\}[Al_2](Si_3)O_{12}$, respectively, where triangular dodecahedral {X}, octahedral [Y], and tetrahedral (Z) notations represent the three special crystallographic cation sites and their polyhedral coordination in space group $Ia\bar{3}d$. Garnet is a remarkable phase in a number of ways and much research in the Earth sciences has focused on the different rock-forming species of this group (Geiger 2013a). A crystal-chemical aspect of significance is the eight-fold or triangular dodecahedral coordination of Fe^{2+} (d^6) and Mn^{2+} (d^5) by oxygen anions and the various physical properties arising from this. Both cations are more typically bonded to six oxygens in an octahedral coordination environment in the crystal structures of many oxides and silicates of the crust or upper mantle.

Different types of electronic transitions in garnet, as expressed in the NIR/Vis/UV regions of the electromagnetic spectrum, can result from the Fe^{2+} and Mn^{2+} cations. The transitions can be studied by optical absorption spectroscopy and they give information on chemical bonding. There have been a number of spectroscopic investigations made to understand the electronic transitions and bonding in almandine- and spessartine-bearing garnets (e.g., Clark 1957; Manning 1967; 1972; Slack and Chrenko 1971; Moore and White 1972; White and Moore 1972; Runciman and Sengupta 1974; Runciman and Marshall 1975; Smith and Langer 1983; Geiger and Rossman 1994; Geiger et al. 2000; Taran et al. 2002; Khomenko et al. 2002; Taran et al. 2007; Krambrock et al. 2013; Platonov and Taran 2018). Computational and theoretical studies relating to the Fe^{2+} spin-forbidden (Zhou and Zhao 1984; Guo-Yin and Min-Guang 1984) and spin-allowed (Newman et al. 1978; Geiger et al. 2003) electronic transitions and their energies have been made. A lot has been learned over the years, but many spectroscopic and crystal-chemical issues are not understood and much remains to be done.

111

112 In our UV/Vis spectroscopic investigation of almandine-pyrope ($Mg_3Al_2Si_3O_{12}$) and
113 almandine-spessartine solid solutions (Geiger et al. Part I), we measured a large number of
114 aluminosilicate garnets with different compositions. During the course of this work, it became
115 apparent that the precise nature of some spin-forbidden transitions of Fe^{2+} and Mn^{2+} is not
116 fully understood. In the case of almandine, several weak absorption features of both Fe^{2+} and
117 Fe^{3+} were observed that were not considered in prior published spectroscopic investigations.
118 Prior assignments of a few spin-forbidden transitions are contradictory. A determination of all
119 Mn^{2+} spin-forbidden transitions in spessartine-bearing garnets is also problematic because
120 UV/Vis spectra were only recorded at room temperature. Moreover, it has not been possible to
121 assign the transitions fully (Smith and Langer 1983). Because we studied a series of closely
122 binary almandine-pyrope, $\{Fe^{2+}_{3x}Mg_{3-3x}\}[Al_2](Si_3)O_{12}$, and almandine-spessartine,
123 $\{Fe^{2+}_{3x}Mn^{2+}_{3-3x}\}[Al_2](Si_3)O_{12}$, solid solutions in a systematic and experimentally consistent
124 manner (Geiger et al. Part I), we could use variations in chemistry to better determine certain
125 absorption features. This type of investigation on such well-defined solid-solution systems was
126 not done before. Furthermore, it became apparent that computational investigations
127 concerning the energies and assignments of some spin-forbidden Fe^{2+} electronic transitions
128 (Zhou and Zhao 1984; Guo-Yin and Min-Guang 1984) as well as Fe^{3+} (Wang et al. 1985)
129 contradict one another and also experimentally measured spectra.
130 In this report, we investigate the spin-forbidden transitions of Fe^{2+} in two almandine-
131 bearing garnets (i.e., one almandine and one pyrope crystal) and Mn^{2+} in several
132 compositionally different spessartine-rich crystals using UV/Vis single-crystal absorption
133 spectroscopy. Spectra are measured and deconvoluted as needed. An effort is made to achieve
134 an up-to-date synthesis of older published and our new experimental spectroscopic results.
135 Assignments for the observed and fitted absorption bands are made. A critical analysis is made
136 that considers the number and energies of measured Fe^{2+} spin-forbidden transitions versus

those calculated from the theoretical studies. The spectrum of nearly end-member spessartine was recorded at low temperature (i.e., 78 K) for the first time. The results are used to analyze, adopting crystal field theory and a consideration of the spectra of other Mn^{2+} phases, the various possible Mn^{2+} spin-forbidden electronic transitions. In addition, five spessartine-rich garnets with different $Mn^{2+}/(Mn^{2+} + Fe^{2+})$ ratios, some of whose spectra show unusual and poorly understood absorption features, are examined and discussed. The role of $^{VI}Fe^{3+}$ in the UV/Vis spectra of aluminosilicate garnets is also considered, inasmuch as it often occurs in relatively small concentrations in almandine, pyrope and spessartine.

SAMPLES AND EXPERIMENTAL METHODS

The garnets used in this investigation are described in the first part of our investigation (Geiger et al. - Part I). The spectroscopic set-ups and measurement details are also given in this report. Care was taken to prepare crystal platelets of the necessary thickness in order that various absorption features were correctly recorded.

The deconvolution and curve-fitting analysis of the spectra were done using Jandel Scientific Peakfit 4.11 software. All the spin-forbidden bands were assumed to have Gaussian shapes. Based on our experience, the intense ligand-metal (L-M) charge-transfer (C-T) low-energy absorption edge is best fit using a combination of Gaussian-Lorentzian line shapes.

RESULTS

The UV/Vis single-crystal spectra of two almandine-bearing garnets, one almandine (Lind 3 - $\{Fe^{2+}_{2.05}Mg_{0.91}Ca_{0.03}\}[Al_{2.00}Fe^{3+}_{0.02}Ti^{4+}_{0.01}]Si_{2.99}O_{12}$) and one pyrope (Turtle Land Mine 17405762 - $\{Mg_{2.19}Fe^{2+}_{0.69}Ca_{0.13}\}[Al_{1.90}Fe^{3+}_{0.08}Cr^{3+}_{0.01}Ti^{4+}_{0.01}]Si_{3.00}O_{12}$) and their fits are shown in Figure 1. Spectra of a nearly end-member spessartine (GRR 43 - $\{Mn^{2+}_{2.82}Fe^{2+}_{0.10}\}Al_{2.02}Si_{3.00}O_{12}$), recorded at 78 and 293 K, are shown in Figure 2. Figure 3 shows the spectra of five spessartine-rich crystals with different $Mn^{2+}/(Mn^{2+} + Fe^{2+})$ ratios

(other cations are ignored in this ratio and two samples are of unusual chemistry - see discussion below). All spectra are given in terms of linear absorption coefficient per cm.

DISCUSSION

UV/Vis spectra of almandine-bearing garnet and fitting of spectra

Spin-forbidden Fe^{2+} transitions. We focus our analysis primarily on the various spin-forbidden electronic absorptions of the measured spectra. Consider the spectra of two garnets, one almandine and the other an almandine-bearing pyrope (Fig. 1). The early and wide-ranging experimental spectroscopic investigation of Moore and White (1972) provides a starting point for our analysis. They measured the spectra of a number of different composition silicate garnets including several almandines and some spectra were recorded at 78 K. They labeled, using letters of the alphabet between "a" and "r", their observed bands (spin forbidden ones between 14000 and 27500 cm^{-1}) and attempted to assign the various electronic transitions. Runciman and Marshall (1975) recorded the UV/Vis spectrum of a garnet with about 82 mol % almandine and 2.7 mol % spessartine at 17 K. Most bands narrow and the spectroscopic resolution increases at lower temperatures. Smith and Langer (1983) measured the UV/Vis spectrum of a synthetic almandine crystal and assigned their observed bands.

Our two measured room-temperature spectra are, in large part, in agreement with these published results. We make, though, an up-to-date analysis on the full number of possible bands, their transition assignments and energies and this differs from previous investigations. Some absorption features that were not observed or considered before are described. Our spectroscopic curve fitting reveals new information. We also consider computational studies, published after the three experimental works noted above, that were made to calculate Fe^{2+} electronic transition energies (Zhou and Zhao 1984; Guo-Yin and Min-Guang 1984). Table 1 attempts to summarize the various and extensive experimental and computational results.

The spectra of almandine-bearing garnets show that the lower energy Fe^{2+} spin-forbidden bands d to h are well pronounced (Fig. 1 and see also Fig. 2 in Geiger et al. Part I - submitted). The bands d, e, f and g are broader than those at higher energy. The presence of band i is expressed as a weak high-wavenumber shoulder on the intense band h (band i is more pronounced in spectra of almandine measured at 78 K, Moore and White 1972, and 17 K, Runciman and Marshall 1975). Absorption feature j needs special comment, as it is weak and poorly defined in some garnet spectra. Moore and White (1972) assigned j to a spin-forbidden band of Mn^{2+}. However, it can be observed in the spectra of garnets with no measurable Mn^{2+} (e.g., Lind 3 - Fig. 1). In addition, it can be obtained in curve fits (see below). This weak feature could, therefore, be related to Fe^{2+} (and it is given as j* in Table 1). Bands k and q appear to be weaker in intensity than bands d to g and are best observed in the spectra of almandine-rich garnets. A few almandine spectra (e.g., GRR 3256 - Geiger et al. - Part I) appear to show a weak shoulder on the high-wavenumber edge of band k. Runciman and Marshall (1975) considered this small absorption effect to represent an electronic transition. We do not consider it further. Finally, there appears to be weak absorption occurring between band m and q at about 24200-24300 cm^{-1} (Fig. 1). Moore and White (1972) observed a feature or features (their bands o and p) in this wavenumber region for an almandine garnet recorded at 78 K. They assigned it to a Mn^{2+} spin-forbidden transition(s) (however, the most intense Mn^{2+} spin forbidden band in spessartine, labelled band p by them, occurs between 24300-24600 cm^{-1} - see section on spessartine below). Because we observe this weak feature at 24200-24300 cm^{-1} in spectra of garnets with no measurable Mn^{2+} (e.g., Lind 3 - Fig. 1b), we think it is better assigned to Fe^{2+} (band m' in Table 1).

Runciman and Marshall (1975) consider that 11 bands are present between about 22500 cm^{-1} and 26000 cm^{-1} in their spectrum of a spessartine-poor almandine recorded at 17 K. All of their proposed bands, some of which are weak and often highly overlapping, can neither be observed in our room-temperature spectra nor obtained by curve fitting (see below).

Spin-forbidden Fe^{3+} transitions. Moore and White (1972) assigned their three bands l, m and r (Fig. 1) to spin-forbidden transitions of Fe^{3+} occurring at the octahedral site of garnet (Table 1). Smith and Langer (1983) assigned these bands to Fe^{2+} (Table 1). They assumed apparently that their synthetic almandine crystal was ideal $\{Fe^{2+}_3\}[Al_2](Si_3)O_{12}$, and that it did not contain $^{VI}Fe^{3+}$ (We note that ^{57}Fe Mössbauer spectra of most synthetic almandines show the presence of small amounts of $^{VI}Fe^{3+}$, Geiger unpublished).

Following this, a reevaluation of the various possible Fe^{3+} transitions in almandine-bearing garnet is necessary. Figure 5 shows the Tanabe-Sugano diagram for a cation with the electronic d^5 configuration calculated taking B = 895 cm^{-1} and C ~ 3866 cm^{-1} giving C/B ~ 4.5. We conclude that the split crystal-field independent split transitions $^6A_{2g}$ (^6S) → $^4A_{1g}$, ^4E_g (^4G) give rise to bands l and m. Band r, which is relatively intense, is assigned to $^6A_{2g}$ → ^4E_g (^4D). The transitions $^6A_{2g}$ → $^4T_{1g}$ (^4G) and $^6A_{2g}$ → $^4T_{2g}$ (^4G) may occur at lower energies, but their bands should be broad and very weak (see the spectrum of andradite, $Ca_3{}^{VI}Fe_2{}^{3+}Si_3O_{12}$ - Taran and Langer 2000; Platonov and Taran 2018). At small concentrations of Fe^{3+}, as in many almandine, pyrope and spessartine crystals, these two latter electronic transitions have not been observed to the best of our knowledge. Note also, that the diagram in Figure 5 differs from that, for example, of andradite, where B = 613 and C = 3308 cm^{-1} giving C/B = 5.4 (Platonov and Taran 2018). Therefore, the energies of the l, m- and r-bands measured in the spectra of the almandine-pyrope garnets (Table 1) are lower than those obtained from Figure 5.

Burns (1993) gives, without explanation, the relative energies of Ligand → Metal C-T transitions for different cations as Cr^{3+} > Ti^{3+} > Fe^{2+} > tet. Fe^{3+} > oct. Fe^{3+} > Ti^{4+}. Marfunin (1979 - page 218) states that the band maximum for O^{2-} → Fe^{3+} C-T (apparently for six-fold coordination) should be centered at about 50000 cm^{-1} in the far UV, but that its low-energy edge extends into the visible region. This is important because the intensity of spin-forbidden

241 bands can be increased by "borrowing" intensity from a L → M C-T transition that involves
242 the same cation (e.g., Marfunin 1979; Bersuker 2010). This appears to be the case for the Fe^{3+}
243 spin-forbidden bands in the spectra of almandine-bearing garnets and especially for band r
244 (Fig. 1 and see also spectra in Geiger et al. Part I).
245
246 **High wavenumber $Fe^{2+/3+}$ spin-forbidden transitions in the UV region**. There have been
247 several spectroscopic studies on almandine-bearing garnets that have shown weak absorption
248 features located at energies above about 27500 cm^{-1} (see Table 1) They were not addressed by
249 Moore and White (1972). These weak transitions are difficult to measure experimentally
250 because they are located on the low-energy edge of the extremely intense O(xygen) → M(etal)
251 C-T band, but attempts have been made.
252 Khomenko et al. (2002) noted a band at about 28000 cm^{-1} in a study of various
253 almandine garnets. We label it band s (Table 1). It could possibly be an electronic sextet-
254 quartet transition of Fe^{3+} arising from the ground $^6A_{1g}$ state to the excited $^4T_{1g}$ level originating
255 from the ^4P term (Fig. 5). Spin-forbidden Fe^{3+} electronic transitions originating from the ^2I
256 term generally have a low probability and, to the best of our knowledge, have never been
257 observed in the optical spectra of Fe^{3+}-bearing minerals and compounds.
258 Manning (1967) and Krambock et al. (2013) noted a band at about 29000-29100 cm^{-1}.
259 We labeled it t (Table 1). Sangsawong et al. (2016) and Sripoonjan et al. (2016) noted a band
260 at roughly 29700 cm^{-1} and assigned it to Fe^{3+} and it is labeled u. Runcimen and Marshall
261 (1975) observed three high wavenumber bands (Table 1) in their 17 K spectrum of almandine.
262 We did not observe with certainty any of these weak spin-forbidden bands in our two
263 spectra of almandine-bearing garnets (see also spectra in Geiger et al. - Part I submitted).
264 Further experimental research involving low-temperature spectroscopic measurements could
265 possibly give more clarification and confirmation on these poorly understood higher energy
266 $Fe^{2+/3+}$ spin-forbidden transitions in almandine-bearing garnets.

Deconvolution of almandine-bearing garnet spectra. Because the UV-Vis spectra of almandine-bearing garnets are complex, involving a considerable number of overlapping spin-forbidden bands, curve fitting could provide useful information. Not much has previously been done in this area. An early simple attempt to deconvolute the spectrum of almandine was made by Manning (1972). Taran et al. (2007) also made fits to the spectra of various almandines, but here the emphasis was on understanding an intense intervalence charge transfer band of the type $\{Fe^{2+}\} + [Fe^{3+}] \rightarrow \{Fe^{3+}\} + [Fe^{2+}]$ that dominated much of the visible region.

We undertook a curve-fitting analysis, having available a large number of various garnet spectra (this work and Geiger et al. - Part I), with the intent of gaining further insight into the measured UV/Vis spectra and Fe^{2+} and Fe^{3+} band behavior. Present computer fit programs enable more information to be gleaned from spectra than was obtained prior to roughly 1990. It is surprising that many UV/Vis garnet spectra recorded since then are not deconvoluted. A discussion of the procedure is in order, because it can be partly subjective for several reasons. Subtle experimental issues can come into play.

We note the following: i) Absorption can be affected by the presence of tiny inclusions (solid and liquid) and crystal imperfections (microcracks, surface pits) especially in the higher energy UV/Vis region. They cause increased absorption and the background can thereby be affected in a complex manner, ii) Room-temperature spectra of almandine-bearing garnet do not show the total number of theoretically possible Fe^{2+} spin-forbidden transitions. Some weak transitions can be obscured by stronger ones because of strong multiple-band overlapping (see Fig. 1). Some bands may be essentially obscured or hidden, iii) Curve fitting at higher energies (i.e., roughly above 25000 cm^{-1}) poses a challenge, because the low-energy O-M C-T edge may consist of a combination of overlapping bands having a different physical origin (i.e., $O^{2-} \rightarrow Fe^{2+}$, $O^{2-} \rightarrow Fe^{3+}$, and $O^{2-} \rightarrow Mn^{2+}$ and even possibly in some garnets $O^{2-} \rightarrow Ti^{4+}$). Because the precise nature (i.e., energy and intensity) of these UV electronic transitions is not known

and only a part of the O → M C-T low-energy edge is measurable, any model fit of it is partly subjective. In terms of this investigation, this edge is important because its "tail" has intensity in the higher energy visible region (Fig. 1) and iv) The spectra of some almandines and spessartines show a broad $^{VIII}Fe^{2+} + {}^{VI}Fe^{3+} \rightarrow {}^{VIII}Fe^{3+} + {}^{VI}Fe^{2+}$ IVCT absorption band (Taran et al. 2007; Geiger and Taran submitted). It can be very intense in some cases, dominating the absorption in the visible region with a band maximum centered at roughly 21000-22000 cm^{-1}. Even in the case where this band is weak and not clearly observable in garnet spectra, it could contribute to the overall absorption between about 15000 and 25000 cm^{-1} (i.e., as in the background). It is difficult, if not almost impossible, to determine the presence of this band, a priori, in all spectra.

Consider now several of the most relevant results obtained from our deconvolution exercise (Fig. 1 and Supplementary Table 3). We are, in general, able to account for most of the measured absorption features of our experimental spectra, even weak ones. In other words, the agreement between observation and the model fit is reasonable. There are notable out comes and several issues that need explanation: i) The intensities of many of the different spin-forbidden bands between about 19000 and 28000 cm^{-1} are roughly similar. This is not totally obvious from the measured spectra alone, ii) The deconvolution procedure requires the presence of a band at about 24260 cm^{-1} (labeled as m' in Table 1). Indeed, there is a weak absorption feature in both measured spectra that indicates a possible band at this energy. This feature was not noted in previous published spectroscopic studies on almandine, iii) Curve fitting indicates that band i is broader and more intense than band h, but this does not appear to be the case for the measured spectra, and finally iv) In order to fit the spectra at higher energies, it is necessary to have a band that has no clear expression in the measured spectra (see Fig. 1 band "??" and Table 1). Its peak maximum is different for our two garnet spectra (i.e., for almandine Lind 3 the wavenumber is 25718 cm^{-1} and for pyrope Turtle Lake it is 26340 cm^{-1}). Moreover, the FWHM values of this band are different for the two fits, that is,

319 2243 cm^{-1} vs 1219 cm^{-1} - Supplementary Table 3). We have no explanation for this band and a
320 physical interpretation cannot be made. Its presence may result from the inability to model the
321 intense O → M C-T edge correctly. Taran et al. (2007) proposed that this hypothetical band
322 could be related to a $^6A_{1g} \rightarrow {}^4T_{2g}$ (^4D) transition of $^{VI}Fe^{3+}$ (their Fig. 5). We note that a $^6A_{1g} \rightarrow$
323 $^4T_{2g}$ (^4D) transition is observed in the optical spectra of compounds with octahedrally
324 coordinated Mn^{2+} (e.g., Mehra and Venkateswarlu 1966; Manning 1968; Sviridov et al. 1978).
325 Fe^{3+} and Mn^{2+} have the same electronic configuration, namely d^5.
326
327 **Energies of Fe^{2+} spin-forbidden transitions based on crystal field theory and from**
328 **published model calculations**
329 **Tanabe-Sugano diagrams and crystal field theory.** Tanabe-Sugano diagrams have
330 traditionally been used as the starting point in the analysis of spin-forbidden transitions. They
331 are based on O_h symmetry of a cation's surroundings. The X cation in garnet has, however, D_2
332 point symmetry and, thus, use of these diagrams is a simple approximation when attempting to
333 assign Fe^{2+} and Mn^{2+} electronic transitions. Figure 4 shows the various transition energies for
334 Fe^{2+} of electronic configuration d^6 as a function of the crystal field strength, Dq (i.e., the bond
335 length in a crystal or ligand field model is given by $10Dq = \frac{5\langle r^4\rangle(Z_L e^2)}{3R^5}$, where $\langle r^4\rangle$ is the
336 mean value to the fourth power of the 3d-electron radius, Z_L is the effective ligand charge, R is
337 the mean metal to ligand distance in the coordination polyhedron and e is the charge of the
338 electron (Dunn et al. 1965; Marfunin 1974; Burns 1993). Most of the transitions from the
339 ground ^5E_g state to the different excited levels, originating from the ^{3}H-, ^{3}P-, ^{3}F- and ^{3}G-terms
340 of free ions, do not indicate any large variation in energy as a function of Dq, with the
341 exception of the $^5E_g \rightarrow {}^3T_{1g}$ (^{3}H) transition. Its energy decreases with increasing Dq.
342 The measured energies of different spin-forbidden Fe^{2+} electronic transitions for
343 various composition almandine-pyrope solid solutions are given in Geiger et al. (Part I). Those

that are two- and three-fold degenerate in O_h symmetry split under D_2 into the states A, B_1, B_2 and B_3 and A $\rightarrow$ A transitions are forbidden by symmetry (e.g., Runciman and Sengupta 1974). Because of this symmetry lowering, the number of possible electronic spin-forbidden transitions in garnet increases significantly. Model calculations of a more sophisticated nature than provided by Tanabe-Sugano diagrams are needed to gain proper insight into all possible electronic transitions.

Model Fe^{2+} electronic-transition calculations. Ideally, experimental garnet spectra could be interpreted if the various spin-forbidden electronic transition energies of Fe^{2+} (and Fe^{3+}) could be calculated. There have been several computational studies.

Zhou and Zhao (1984) used a model (i.e., "strong-field scheme of 'once-diagonalization'" that has one adjustable parameter) to calculate a total of 36 different Fe^{2+} transitions. Their energies lie between 12000 and 51000 cm^{-1}. The 12 transitions with energies roughly above 30000 cm^{-1} would be difficult to measure, because they must be superimposed on the intense oxygen $\rightarrow$ metal charge-transfer edge. Here, the absorbance is so high that it is difficult to record spectra experimentally. With this in mind we start our simple analysis. Because the X cation in garnet lies in a field of D_2 symmetry, the ^5E_g level splits into $^5A + {}^5B_1$ levels and ^5A is the ground state. Zhou and Zhao (1984) calculated the energies of various $^5A \rightarrow {}^3B_1$, $\rightarrow {}^3B_2$ and $\rightarrow {}^3B_3$ transitions and concluded "… the results obtained are in quite good agreement with the observed values". Their assignments for different Fe^{2+} electronic transitions are listed in Table 1. There is reasonable agreement between experimental spectra and model for a number of transition energies but not all. Zhou and Zhao (1984) proposed, for example, the existence of transitions at 12232 cm^{-1} and 14986 cm^{-1}, but no bands with these energies have been observed in more recent spectroscopic studies. Furthermore, they did not calculate any transitions having energies between 19154 and 20229 cm^{-1}, although several spin-forbidden bands can be observed in this wavenumber range.

Guo-Yin and Min-Guang (1984) published, in the same year, Fe^{2+} electronic transition energies based on their "superposition" and "point-charge" models (see Table 1). The agreement between their results and those of Zhou and Zhao (1984) is mixed. In terms of experiment and their model results, there are also inconsistencies. For example, Guo-Yin and Min-Guang (1984) assigned band r with a wavenumber of about 27200 cm^{-1} to a number of different electronic transitions of Fe^{2+}. They argued that there are several transitions with energies close to this value (see their Table I) and that this explains the relatively strong intensity and broadness of this measured band in various garnet spectra. In other words, the experimental band r should represent a number of closely overlapped Fe^{2+} electronic transitions. We think, however, that this absorption feature is better assigned to $^{VI}Fe^{3+}$, as originally done by Moore and White (1972). Guo-Yin and Min-Guang also argued, contrary to the spectroscopic results and analysis of Moore and White (1972) and other published works, as well as our present investigation, that three measured transitions at 23700, 24300 and 24500 cm^{-1} are related to Fe^{2+} and not Mn^{2+}. This proposal is problematic, as discussed below in the section on the UV/Vis spectra of spessartine and its spin-forbidden Mn^{2+} transitions.

Finally, in a third computational study, Wang et al. (1985) calculated transition energies for Fe^{3+} in silicate garnet. They compared their model energies to the absorption bands observed in the spectra of grossular, spessartine, and almandine. They calculated, for example, a wavenumber of 27284 cm^{-1} for band r and assigned it to the transition $^6A_1 \rightarrow {}^4B_2$ for Fe^{3+} located at the{X} site of garnet (cf. Table 1). We cannot, however, agree with their assignment, because we are not aware of any experimental results that unambiguously show significant amounts of Fe^{3+} at {X}.

The UV/Vis spectra of spessartine

Spin-forbidden Mn^{2+} transitions. Manning (1967) and Moore and White (1972) measured the UV/Vis single-crystal spectra of several natural spessartines and made assignments for

396 several spin-forbidden Mn^{2+} bands. Smith and Langer (1983) studied synthetic end-member
397 spessartine and also made an analysis of the electronic transtions. They reported more bands
398 than the former two studies. Table 2 lists measured spin-forbidden Mn^{2+} absorption bands and
399 their energies for various natural spessartine-rich garnets and the synthetic crystal. The
400 number of observed bands differs among the published works. Attempts made to interpret and
401 assign the various Mn^{2+} transtions have not been fully successful. For example, Smith and
402 Langer (1983) made an analysis using their synthetic spessartine that should not, unlike most
403 natural crystals, have contained other transition metals in amounts great enough to lead to
404 absorption bands. They discussed the difficulty in assigning all their measured Mn^{2+} bands
405 using a Tanabe-Sugano diagram for O_h symmetry. Considering the various issues and
406 uncertainties, we studied the UV/Vis spectra of several natural spessartine-rich crystals of
407 different composition.

408 The spectra of a nearly end-member spessartine (sample GRR 43 - composition
409 Sps97Alm3) measured at room and liquid nitrogen temperature are shown in Figure 2. The
410 different spin-forbidden Mn^{2+} transition energies are given in Table 2. At room temperature,
411 the spectrum shows a number of well-resolved bands. Those below about 22000 cm^{-1} appear
412 to be broader than those between 22000 and 25000 cm^{-1}. These bands are narrower and lie at
413 lower energies in the spectrum recorded at 78 K. The bands below 24400 cm^{-1} tend to show
414 greater energy shifts upon cooling than those at higher wavenumbers. Bands p and o are
415 clearly pronounced at 78 K and band n splits into two components with maxima at ~23630 and
416 23830 cm^{-1} upon cooling. In addition, in the spectrum collected at 78 K, four more possible
417 bands appear on the O $\rightarrow$ M C-T edge between 25000 and 30000 cm^{-1} and at least three bands
418 at lower wavenumbers between 22000 and 15000 cm^{-1} compared to the RT spectrum.
419
420 **Spessartine crystal chemistry and a crystal field analysis of its spin-forbidden Mn^{2+}**
421 **transitions.** The crystal structure of end-member synthetic spessartine was studied at 100 K,

This is the peer-reviewed, final accepted version for American Mineralogist, published by the Mineralogical Society of America.
The published version is subject to change. Cite as Authors (Year) Title. American Mineralogist, in press.
DOI: https://doi.org/10.2138/am-2022-8500. http://www.minsocam.org/

293 K and 500 K (Geiger and Armbruster 1997). A notable property of the $\{X^{2+}\}$ cation in garnet is its marked anisotropic vibrational behavior, as is the case for Mn^{2+} in spessartine. There are two crystallographically independent Mn^{2+}-O bonds. The shorter Mn^{2+}-O(2) bond shows no measurable change in length between 293 K and 100 K (i.e., 2.245(1) Å), whereas the longer Mn^{2+}-O(4) bond shows a very slight decrease from 2.404(1) to 2.399(1) Å.

How are the various electronic transitions of Mn^{2+} (Fig. 2 and Table 2) to be interpreted? We start by considering the Tanabe-Sugano diagram for a cation with a d^5 configuration (Fig. 5). The local field bond strength for Mn^{2+} in spessartine is given by $Dq_{cubic} = 8/9Dq_{octahedral}$ in the crystal-field model (e.g., Marfunin 1974; Burns 1993). Therefore, one may assume, as a starting point and in a simple approximation, that the energies of the Mn^{2+} bands for both coordination environments should not be too different. The lowest wavenumber Mn^{2+} transitions from the ground $^6A_{1g}$ state are $^4T_{1g}$ (^4G) and $^4T_{2g}$ (^4G) for O_h symmetry. They can split into three further states for D_2, but a transition to the excited $^4A_1$ state, originating from the $^4T_{2g}$ (^4G) level, is forbidden by selection rules (Marfunin 1974). Therefore, the maximum number of possible Mn^{2+} bands should not be greater than five. The number of observed bands between 22000 and 15000 cm^{-1} at 78 K is, counting shoulders, at least seven (Fig. 2 and Table 2).

Following this, we consider the UV/Vis spectra of a number of Mn^{2+}-containing crystals and compounds in order to obtain more spectroscopic insight. Mn^{2+} is often octahedrally coordinated by ligands such as F^-, Cl^-, Br^-, I^-, S^{2-} or H_2O, as discussed in a number of investigations (e.g., Mehra and Venkateswarlu 1966; McPherson et al. 1974; Sviridov et al. 1978; Taralatra and Mukherjee 1989; Caldiñoand Rubio 1993; Hernández et al. 1999; Saleh et al. 2019). There are also spectroscopic investigations on Mn^{2+} silicates such as rhodonite (Manning 1968; Marshall and Ruciman 1975) and pyroxmangite, bustamite, and serandite (Manning 1967).

This is the peer-reviewed, final accepted version for American Mineralogist, published by the Mineralogical Society of America.
The published version is subject to change. Cite as Authors (Year) Title. American Mineralogist, in press.
DOI: https://doi.org/10.2138/am-2022-8500. http://www.minsocam.org/

Mn^{2+} gives rise only to spin-forbidden transitions and they are typically observed at wavenumbers above 20000 cm^{-1} (The $^6A_{1g} \rightarrow {}^4T_{2g}$ (^4G) and $^6A_{1g} \rightarrow {}^4T_{1g}$ (^4G) bands for Mn^{2+} are generally located at higher energies compared to those for Fe^{3+}, because Mn^{2+} has a lower crystal field strength - Marfunin 1979). The UV/Vis spectra of the various compounds noted above typically show sharp and distinct bands. Those occurring at energies between 23000 and 25000 cm^{-1} are generally assigned to the crystal-field-independent transition $^6A_{1g} \rightarrow {}^4A_{1g}$, ^4E_g (^4G). Bands located between 27000 and 30000 cm^{-1} are assigned to the transition $^6A_{1g} \rightarrow {}^4E_g$ (^4D).

In terms of the spectrum of spessartine, Manning (1967) assigned the relatively strong absorption doublet with wavenumbers of approximately 24000 and 24500 cm^{-1} (the o and p bands given later by Moore and White 1972 - Table 2) to split components of the crystal-field-independent transition $^6A_{1g}$ (^6S) $\rightarrow {}^4A_{1g}$ (^4G), ^4E_g (^4G). The two weaker bands at about 23500 cm^{-1} (band n) and 20800 cm^{-1} (band j) were assigned to $^6A_{1g} \rightarrow {}^4T_{2g}$ (^4G) and $^6A_{1g} \rightarrow {}^4T_{1g}$ (^4G), respectively. Various questions arise. First, the spin-allowed $^5E_g \rightarrow {}^5T_{2g}$ transitions of $^{VIII}Fe^{2+}$ in almandine show a strong splitting of nearly 2000 cm^{-1} (e.g., Geiger and Rossman 1994). However, the splitting of the spin-forbidden transition $^6A_{1g} \rightarrow {}^4A_{1g}$, ^4E_g of Mn^{2+} is less than two hundred cm^{-1}. It is expected that the transition splittings for Fe^{2+} and Mn^{2+} in garnet should not be too dissimilar. Therefore, we think that the four observed bands between 18000 and 22000 cm^{-1} in the RT spectrum of spessartine (Fig. 2) are components of the split $^6A_{1g} \rightarrow {}^4T_{1g}$ (^4G) and $^6A_{1g} \rightarrow {}^4T_{2g}$ (^4G) transitions. They lie at lower wavenumbers compared to the interpretation of Manning (1967). Second, the five bands observed between 23000 and 25000 cm^{-1} in the 78 K spectrum (Fig. 2) are narrow. Therefore, one may assume that they originate from the split $^6A_{1g} \rightarrow {}^4A_{1g}$, ^4E_g (^4G) transition. Indeed, the low-temperature spectrum of $^{VI}Mn^{2+}$-bearing $CdC1_2$ (Ramírez-Serrano et al. 1997), as well as the spectra of a series of Mn^{2+} salts (Lohr and McClure1968), show similar spectroscopic fine structure for the $^6A_{1g} \rightarrow {}^4A_{1g}$,

472 ^4E_g (^4G) transition. However, the reason for this is not understood. Goode (1963) concluded,
473 based on a study of a series of Mn^{2+}-bearing amines and hydrates, that spin-orbit interactions
474 cannot account for the spectral fine structure.

475 We note that the spectrum of Mn^{2+}-doped KCl, where Mn^{2+} is in eight-fold
476 coordination (Sviridov et al. 1976), is simpler compared to that of spessartine. At room
477 temperature, the spectrum shows six relatively broad absorption bands between 20000 to
478 30000 cm^{-1}. They were assigned to transitions from the $^6A_1$ (^6S) ground state to various excited
479 quartet levels in the cubic field (Mehra and Venkateswarlu 1966). Compared to the spectrum
480 of spessartine, less band splitting is observed.

481 Finally, we consider possible transition assignments for the weak spin-forbidden bands
482 at the highest wavenumbers above roughly 26000 cm^{-1} in the 78 K spectrum of spessartine
483 (Fig. 2). Five bands, three of which are weak in intensity and therefore a bit questionable, are
484 superimposed on the intense O-M C-T absorption edge. The narrow and most intense band at
485 about 28990 cm^{-1} could possibly derive from the $^6A_{1g} \rightarrow {}^4E_g$ (^4D) transition under D_2
486 symmetry. A ^4E_g (^4D) transition with this approximate energy is observed in the spectra of a
487 series of manganese halides (Sviridov et al. 1978), where the Mn^{2+} ions are in octahedral
488 coordination. The other four Mn^{2+} bands in spessartine could arise through transitions to one
489 of the excited quartet states $^4T_{1g}$ (^4D), ^4E_g (^4D) and $^4T_{1g}$ (^4P) (Fig 5) also split in D_2 symmetry.

490 To summarize, it is difficult to interpret spessartine's UV/Vis spectrum and the various
491 spin-forbidden Mn^{2+} bands in a clear and self-consistent manner. It appears that crystal field
492 theory and the use of Tanabe-Sugano diagrams are insufficient to explain all the observed
493 transitions. Smith and Langer (1983) came to a similar conclusion.

494

495 **Spessartines of "unusual" composition and other spectroscopic behavior.** We analyze,
496 here, the spectra of several additional spessartine-rich garnets (Fig. 3), especially two crystals
497 of unusual composition, because they show interesting absorption features. Consider first the

498 spectrum of sample Lind 2 of composition
499 $(Mn_{2.44}Fe_{0.14}Mg_{0.37}Ca_{0.04})[Al_{1.99}Fe_{0.01}Ti_{0.01}]Si_{2.99}O_{12}$. It shows high absorption above 22000
500 cm^{-1} for both the spin-forbidden Mn^{2+} bands and the O → M C-T edge. The $O^{2-} \rightarrow {}^{VI}Mn^{2+}$ C-T
501 band in crystals is located just in the UV region according to Marfunin (1979 - apparently for
502 six-fold coordinated Mn^{2+}). If similar behavior is the case for $O^{2-} \rightarrow {}^{VIII}Mn^{2+}$ C-T in
503 spessartine, the relatively strong intensities of the spin-forbidden bands of Mn^{2+} located
504 between 25,000 and 23,000 cm^{-1} cannot be explained through an interaction with $O^{2-} \rightarrow$
505 $^{VIII}Mn^{2+}$ C-T. The weak intensities of the highest wavenumber Mn^{2+} spin-forbidden bands
506 above 26,000 cm^{-1} (Fig. 2) would argue against this. It is difficult to explain the high-
507 intensities of both the C-T edge and the spin-forbidden Mn^{2+} bands between 25,000 and
508 23,000 cm^{-1}. It must be noted that spessartine Lind 2 contains three different transtion metals
509 and Fe occurs at two different structural sites and with two different oxidation states. In terms
510 of the C-T edge, it may be composite in nature consisting of overlapping $O^{2-} \rightarrow {}^{VIII}Mn^{2+}$, O^{2-}
511 $\rightarrow {}^{VIII}Fe^{2+}$, $O^{2-} \rightarrow {}^{VI}Fe^{3+}$ and $O^{2-} \rightarrow {}^{VI}Ti^{4+}$ transtions, but this is just speculation.
512 The spectrum of spessartine MMUR 32999/912 also appears a bit different compared
513 to the others samples in Fig. 3. Its O → M C-T edge is also relatively intense and, in addition,
514 the spin-forbidden bands of Mn^{2+} are broad. This garnet has the composition
515 $\{Mn^{2+}_{2.87}Fe^{2+}_{0.09}Ca_{0.04}\}[Al_{1.94}Fe^{3+}_{0.06}](SiO_4)_{2.52}(OH_{1.11},F_{0.81})$, where both F^- and OH^- are
516 thought to substitute for O^{2-} at the general x, y, z crystallographic site in garnet (Boiocchi et al.
517 2012). Thus, there are three different types of ligands that could bond to Mn^{2+}. Because of
518 this, the d-electronic transition energies of Mn^{2+} could be slightly different locally. Broadening
519 of the spin-forbidden Mn^{2+} bands could result.
520 Finally, the spectra of both of these spessartines show an absorption feature located at
521 slightly lower energies than band n' and labled as ?. It does not appear in the spectra of other
522 spessartines or it is much less pronounced. We do not have a good explanation for this feature.
523

IMPLICATIONS

What are some implications deriving from this study? It is well known that crystal field theory is incomplete in terms of describing chemical bonding quantitatively. Moreover, the use of Tanabe-Sugano diagrams to interpret Fe^{2+} and Mn^{2+} spin-forbidden electronic transitions, occurring in the triangular dodecahdrally coordinated site in garnet, is fraught with uncertainty. Together, this leads to problems interpreting fully and quantitatively the UV/Vis spectra of almandine and especially spessartine. More sophisticated, yet still model-dependent, calculations also appear inadequate in explaining fully the Fe^{2+} and Fe^{3+} spin-forbidden transitions in garnet. There exists little work on analyzing the absorption spectra of complex silicates using more quantitative bonding theories. State-of-the-art computational and theoretical investigations are needed to better interpret various spectroscopic results and, here, UV/Vis absorption spectra are a good case in point. Electronic structure calculations on end-member spessartine and almandine should be possible. Full, more quantitative investigations of Fe^{2+} and Mn^{2+} electronic transitions need to be made. Based on the experimental spectra of almandine and spessartine, their electronic transitions should be quite different in behavior. Both cations show anisotropic vibrational behavior (Geiger et al. 1992; Geiger and Armbruster 1997) and their potentials can be expected to be rather anharmonic (Geiger 2013b), thus complicating crystal chemical and electronic transition behavior.

Second, there is little understanding of the nature of the low-energy $O \rightarrow M$ charge-transfer edge in the spectra of transition-metal-bearing silicate garnets. Most natural garnets contain more than one transition metal and in the case of the elements iron and manganese they can also be in different valence states.

Finally, it is rather surprising, in spite of decades of experimental research, that UV/Vis spectra on silicates recorded at low temperatures (cf., Runciman and Marshall 1975) are far from being sufficient to understand electronic transition behavior. At room temperature, bands are broader and thermal effects often obscure spectral fine structure. More complete and

quantitative absorption spectra are necessary to obtain a better understanding behind electronic-transition and chemical-bonding behavior in garnet.

ACKNOWLEDGMENTS

A number of garnet samples used in this study were obtained from several different sources. They are given in Geiger et al. (Part I). We thank the various institutions and individuals for their generosity. This research was supported by a grant to C.A.G. from the Austrian Science Fund (FWF: P 30977-NBL). He also thanks the "Land Salzburg" for financial support through the initiative "Wissenschafts- und Innovationsstrategie Salzburg 2025".

559 **REFERENCES CITED**

560

561 Bersuker, I.B. (2010) Electronic Structure and Properties of Transition Metal Compounds:
562 Introduction to the Theory. 2nd ed., John Wiley and Sons. 759 p.
563 Boiocchi, M., Bellatreccia, F., Della Ventura, G., and Oberti, R. (2012) On the symmetry and atomic
564 ordering in (OH,F)-rich spessartine: towards a new hydrogarnet end-member. Zeitschrift für
565 Kristallographie, 227, 385-395.
566 Burns, R.G. (1970; 1993) Mineralogical Applications of Crystal Field Theory. First (1970) and
567 Second (1993) editions. Cambridge University Press, Cambridge, England. 551 p.
568 Caldiño, G.U. and Rubio, O.J. (1993) Optical spectroscopy of Mn^{2+} ions in $CaCl_2$ single crystals.
569 Radiation Effects and Defects in Solids, 127, 83-91.
570 Clark, S.P., Jr. (1957) Absorption spectra of some silicates in the visible and near infrared. American
571 Mineralogist, 42, 732-742.
572 Geiger, C.A. (2004) Spectroscopic investigations relating to the structural, crystal-chemical and
573 lattice-dynamic properties of $(Fe^{2+}, Mn^{2+}, Mg, Ca)_3Al_2Si_3O_{12}$ garnet: A review and analysis. In
574 European Notes in Mineralogy - Spectroscopic Methods in Mineralogy, E. Libowitzky and A.
575 Beran, Eds., v. 6, 589-645.
576 Geiger, C.A. (2008) Silicate garnet: A micro to macroscopic (re)view. American Mineralogist, 93,
577 360-372.
578 Geiger, C.A. (2013a) Garnet: A key phase in nature, the laboratory and in technology. Elements, 9,
579 447-452.
580 Geiger, C.A. (2013b) Static disorders of atoms and experimental determination of Debye temperature
581 in pyrope: Low- and high-temperature single-crystal X-ray diffraction study -- Discussion.
582 American Mineralogist, 98, 780-782.
583 Geiger, C.A. (2016) A tale of two garnets: The role of solid solution in the development toward a
584 modern mineralogy. American Mineralogist, 101, 1735-1749.

585 Geiger, C.A. and Feenstra, A. (1997) Molar volumes of mixing of almandine-pyrope and almandine-
586 spessartine garnets and the crystal chemistry of aluminosilicate garnets. American
587 Mineralogist, 82, 571-581.
588 Geiger, C.A. and Rossman, G.R. (1994) Crystal field stabilization energies of almandine-pyrope and
589 almandine-spessartine garnets determined by FTIR near infrared measurements. Physics and
590 Chemistry of Minerals, 21, 516-525.
591 Geiger, C.A. and Armbruster, T. (1997) $Mn_3Al_2Si_3O_{12}$ spessartine and $Ca_3Al_2Si_3O_{12}$ grossular garnet:
592 dynamical structural and thermodynamic properties. American Mineralogist, 82, 740-747.
593 Geiger, C.A., Stahl, A., and Rossman, G.R. (2000) Single-crystal IR- and UV/VIS-spectroscopic
594 measurements on transition-metal-bearing pyrope: The incorporation of hydroxyl in garnet.
595 European Journal of Mineralogy, 12, 259-271.
596 Geiger, C.A., Grodzicki, M., and Amthauer, G. (2003) The crystal chemistry and Fe^{II} site properties
597 of aluminosilicate garnet solid solutions as revealed by Mössbauer spectroscopy and electronic
598 structure calculations. Physics and Chemistry of Minerals, 30, 280-292.
599 Geiger, C.A., Taran, M.N. and Rossman, G.R. (in press) UV/Vis single-crystal spectroscopic
600 investigation of almandine-pyrope and almandine-spessartine solid solutions: Part I. Spin-
601 forbidden electronic transition energies, bonding and crystal chemistry. American
602 Mineralogist.
603 Geiger, C.A., Armbruster, Th., Lager, G.A., Jiang, K., Lottermoser, W., and Amthauer, G. (1992) A
604 combined temperature dependent Mössbauer and single crystal X-ray diffraction study of
605 synthetic almandine: Evidence for the Gol`danskii-Karyagin effect. Physics and Chemistry of
606 Minerals, 19, 121-126.
607 Guo-Yin, S. and Min-Guang Z. (1984) Analysis of the spectrum of Fe^{2+} in Fe-pyrope garnets.
608 Physical Review B, 30, 3691-3703.

Hernández, F.D., Rodìguez, F., Moreno, M., and Güdel, H.U. (1999) Pressure dependence of the crystal field spectrum of the NH_4MnCl_3 perovskite: correlation between 10Dq, Ne and Nt, and the Mn-Cl distance in $MnCl_4^{6-}$ complexes. Physica B, 265, 186-190.

Khomenko, V.M., Langer, K., Wirth, R., and Weyer, B. (2002) Mie scattering and charge transfer phenomena as causes of the UV edge in the absorption spectra of natural and synthetic almandine garnets. Physics and Chemistry of Minerals, 29, 201-209.

Krambrock, K., Guimarães, F.S., Pinheiro, M.V.B., Paniago, R., Righi, A., Persiano, A.I.C., Karfunkel, J. and Hoover, D.B. (2013) Purplish-red almandine garnets with alexandrite-like effect: causes of colors and color-enhancing treatments. Physics and Chemistry of Minerals, 40, 555-562.

Laurs, B.M. and Knox, K. (2001) Spessartine garnet from Ramona, San Diego County, California. Gems and Gemology, 37, no. 4, 278-295.

Manning, P.G. (1968) Absorption spectra of the manganese-bearing chain silicates pyroxmangite, rhodonite, bustamite and serandite. Canadian Mineralogist, 9, 348-357.

Manning, P.G. (1967) The optical absorption spectra of the garnets almandine-pyrope, pyrope, and spessartine and some structural interpretations of mineralogical significance. Canadian Mineralogist, 9, 237-251.

Manning, P.G. (1972) Optical absorption spectra of Fe^{3+} in octahedral and tetrahedral sites in natural garnets. Canadian Mineralogist, 11, 826-839.

Marfunin, A.S. (1979) Physics of mineral and inorganic materials. Springer. Berlin. 340 p.

McPherson, G.L., Aldrich, H.S. and Chang, J.R. (1974) Electronic spectrum and magnetic properties of $CsMnBr_3$. Journal of Chemical Physics, 60, 534-537.

Marshall, M. & Runciman, W.A. (1975) The absorption spectrum of rhodonite. American Mineralogist, 60, 88-97.

Mehra, A. and Venkateswarlu, P. (1966) Absorption Spectrum of Mn^{2+} in KCl. Journal of Chemical Physics, 45, 3381-3383.

635 Moore, R.K. and White, W.B. (1972) Electronic spectra of transition metal ions in silicate garnets.
636 Canadian Mineralogist, 11, 791-811.
637 Newman, D.J., Price, D.D., and Runciman, W.A. (1978) Superposition model analysis of the near
638 infrared spectrum of Fe^{2+} in pyrope-almandine garnets. American Mineralogist, 63, 1278-
639 1281.
640 Platonov, A.N. and Taran, M.N. (2018) Optical spectra and color of natural garnets. Naukova dumka,
641 Kiev (in Russian). 255 p.
642 Runciman, W.A. and Marshall, M. (1975) The magnetic circular dichroism of pyrope-almandine
643 garnets. American Mineralogist, 60, 1122-1124.
644 Runciman, W.A. and Sengupta, D. (1974) The spectrum of Fe^{2+} ions in silicate garnets. American
645 Mineralogist, 59, 563-566.
646 Saleh, M.A., Nugroho, A.A., Dewi, K.K., Supand, A.R., Onggo, D., Kuhn, H., and van Loosdrecht,
647 P.H.M. (2019) Optical absorption spectra of Mn^{2+} in of $(C_6H_5CH_2CH_2NH_3)_2$-$MnCl_4$ and
648 $(NH_2CH_2CH_2NH_2)_2$-$MnCl_4$ hybrid compounds. Key Engineering Materials, 811, 179-183.
649 Slack, G.A. and Chrenko, R.M. (1971) Optical absorption of natural garnets from 1000 to 30000
650 wavenumbers. Journal of Optical Society of America, 61, 1325-1329.
651 Smith, G. and Langer, K. (1983) High pressure spectra up to 120 kbars of the synthetic garnet end
652 members spessartine and almandine. Neues Jahrbuch für Mineralogie - Monatshefte, 12, 541-
653 555.
654 Sripoonjan, T., Maneekrajangsaeng, M., Jakkawanvibul J., and Leelawatanasuk, T. (2016) A new
655 “purple rhodolite” garnet from Mozambique: Its characteristics and properties. Conference
656 GIT2016, 77-83.
657 Sviridov, D.T., Sviridova, R.K., Kulik, N.I., and Glasko, V.B. (1978) Investigation of the optical
658 spectra of crystals containing Mn^{2+} ions. Journal of Spectroscopy, 29, 1399-1400.
659 Sviridov, D.T., Sviridova, R.K., Smirnov Yu. F. (1976) Optical spectra of transition metal ions in
660 crystals. Moscow, Nauka, 266 p. (in Russian).

Taralatra, J. and Mukherjee, R.K. (1989) Optical studies of electronic transitions of Mn^{2+} ion in $Na_2Mn_3Cl_8$ single crystals. Physica Status Solidi (B), 155, 541-548.

Taran, M.N. and Langer, K. (2000) Electronic absorption spectra of Fe^{3+} in andradite and epidote at different temperatures and pressures. European Journal of Mineralogy, 12, 7-15.

Taran, M.N, Langer, K., and Geiger, C.A. (2002) Single-crystal electronic absorption spectroscopy on chromium, cobalt and vanadium-bearing synthetic pyropes at different temperatures and pressures. Physics and Chemistry of Minerals, 29, 362-368.

Taran, M.N., Dyar, M.D. and Matsuyk, S.S. (2007) Optical absorption study of natural garnets of almandine-skiagite composition showing intervalence $Fe^{2+} + Fe^{3+} \rightarrow Fe^{3+} + Fe^{2+}$ charge-transfer transition. American Mineralogist, 92, 753-760.

Wang, H.-S., Zhao, S.-B. and Xiao T.-B. (1985) Energy matrices of irreducible representations of point group D_2 for electron system d^5 and the electronic spectrum of ion Fe^{3+} in silicate garnets. Journal of Physics C: Solid State Physics, 18, 563-567.

White W.B. and Moore R.K. (1972) Interpretation of the spin-allowed bands of Fe^{2+} in silicate garnets. American Mineralogist, 57, 1692-1710.

Zhou, K-W. and Zhao, S-B. (1984) The spin-forbidden spectrum of Fe^{2+} in silicate garnets. Journal of Physics C: Solid State Physics, 17, 4625-4632.

This is the peer-reviewed, final accepted version for American Mineralogist, published by the Mineralogical Society of America.
The published version is subject to change. Cite as Authors (Year) Title. American Mineralogist, in press.
DOI: https://doi.org/10.2138/am-2022-8500. http://www.minsocam.org/

678

679 Table 1. Fe^{2+} and Fe^{3+} electronic transitions for various almandines described by their band labels and wavenumbers, $\tilde{\nu}$, as measured by single-crystal
680 UV/Vis/NIR spectroscopy and from model calculations. Band labels "a" to "r" and their energy ranges for several natural almandine garnets are from
681 White and Moore (1972)$^{\diamond}$ and Moore and White (1972)§ recorded at room temperature and for one almandine at 78 K. Runciman and Marshall (1975)$^{\otimes}$
682 measured the spectrum of a natural almandine at 17 K. The wavenumbers for synthetic almandine are from Geiger and Rossman (1994)* and Smith and
683 Langer (1983)$^{\#}$. Bands a, b and c are spin-allowed transitions and those at higher wavenumbers are spin-forbidden transitions, excepting the IVCT band.
684 Bands labelled j*, IVCT, m′, and "??" are from this work^{TW}. Cation and site assignment refers to either Fe^{2+} or Fe^{3+} and their coordination in garnet as
685 taken from the literature and proposed in this work (those given in parentheses are from published studies and are probably incorrect). The second column
686 from the right-hand-side lists assignments for the spin-allowed transitions of $^{VIII}Fe^{2+}$ according Newman et al. (1978)$^{\varnothing}$ and spin-forbidden transitions of
687 $^{VIII}Fe^{2+}$ and $^{VI}Fe^{3+}$ (l, m and r) from Moore and White (1972)§, Zhou and Zhao (1984)$^{\oplus}$ and this work^{TW}. Guo-Yin and Min-Guang (1984)$^{\blacklozenge}$ calculated
688 electronic transitions of $^{VIII}Fe^{2+}$ and they are given in those cases where the wavenumber appears to match experimental band energies. Wang et al.
689 (1985) calculated transition energies assuming the presence of $^{VIII}Fe^{3+}$ (see text).

Band Label$^{\diamond, \S, TW}$	$\tilde{\nu}$ (nat.) (cm^{-1})$^{\diamond, \S, TW}$	$\tilde{\nu}$ (nat.) 78 K (cm^{-1})§	$\tilde{\nu}$ (nat.) 17 K (cm^{-1})$^{\otimes}$	$\tilde{\nu}$ (syn.) (cm^{-1})*,$^{\#}$	Cation & Site Assignment	Electronic Transition$^{\varnothing, \oplus, \S, TW}$	Electronic Transition$^{\blacklozenge}$
a	4303-4390	-	-	4317*/-	$^{VIII}Fe^{2+}$	$^5A \rightarrow {}^5B_3{}^{\varnothing}$	$^5A_1 \rightarrow {}^5B_3$ (D)
b	5868-6011	-	-	5733*/5800$^{\#}$	$^{VIII}Fe^{2+}$	$^5A \rightarrow {}^5A^{\varnothing}$	$^5A_1 \rightarrow {}^5A_1$ (D)
c	7633-7770	-	-	7564*/7600$^{\#}$	$^{VIII}Fe^{2+}$	$^5A \rightarrow {}^5B_2{}^{\varnothing}$	$^5A_1 \rightarrow {}^5B_2$ (D)
d	~14750-14250	14278	14280	14400$^{\#}$	$^{VIII}Fe^{2+}$	$^5A \rightarrow {}^3B_2{}^{\oplus}$	$^5A_1 \rightarrow {}^3B_3$ (H)
e	~16770-16150	16300	16160	16200$^{\#}$	$^{VIII}Fe^{2+}$	$^5A \rightarrow {}^3B_1{}^{\oplus}$	$^5A_1 \rightarrow {}^3B_1$ (H)
f	~17700-17300	17473	17240	17600$^{\#}$	$^{VIII}Fe^{2+}$	$^5A \rightarrow {}^3B_2{}^{\oplus}$	$^5A_1 \rightarrow {}^3B_2$ (H)
g	~19300-19100	19176	18950	19100$^{\#}$	$^{VIII}Fe^{2+}$	$^5A \rightarrow {}^3B_1{}^{\oplus}$	$^5A_1 \rightarrow {}^3B_2$ (H)
h	~19900-19800	19841	19760	19900$^{\#}$	$^{VIII}Fe^{2+}$	$^5A \rightarrow {}^3B_3{}^{\oplus}$	$^5A_1 \rightarrow {}^3B_1$ (H)
i	~20100-20300	20088	20120	-	$^{VIII}Fe^{2+}$	$^5A \rightarrow {}^3B_3{}^{\oplus}$	$^5A_1 \rightarrow {}^3A_1$ (H),

This is the peer-reviewed, final accepted version for American Mineralogist, published by the Mineralogical Society of America.
The published version is subject to change. Cite as Authors (Year) Title. American Mineralogist, in press.
DOI: https://doi.org/10.2138/am-2022-8500. http://www.minsocam.org/

						$^5A \rightarrow {}^3B_1{}^{\oplus}$	$^5A_1 \rightarrow {}^3A_1$ (F)
j*/j	~20800	-	-	-	$^{VIII}Fe^{2+}$ (Mn^{2+})[§]	$^5A \rightarrow {}^3B_3{}^{\oplus}$	$^5A_1 \rightarrow {}^3B_3$ (H)
IVCT band[$]	~21100 Broad	-	-	-	$^{VIII}Fe^{2+}$-$^{VI}Fe^{3+}$	IVCT $^{VIII}Fe^{2+} \rightarrow {}^{VI}Fe^{3+}$ [$, TW]	-
k	21800-21600	21636	21650	21800[#]	$^{VIII}Fe^{2+}$	$^5A \rightarrow {}^3B_3{}^{\oplus}$	$^5A_1 \rightarrow {}^3B_1$ (P)
l	~22840-22878	22878	22770	-	$^{VI}Fe^{3+}$ ($^{VIII}Fe^{2+}$)[#]	split $^6A_{1g} \rightarrow {}^4A_{1g}$, ^4E_g (^4G)[§]	$^5A_1 \rightarrow {}^3B_1$ (F), $^3B_3$ (F)
m	~23300-24600	23337	23285	23200[#]	$^{VI}Fe^{3+}$		Fe^{3+}
m′	~24217	-	-	-	$^{VIII}Fe^{2+}$	$^5A \rightarrow {}^3B_3{}^{\oplus}$ results by fitting[TW]	
q	~25000	25025	-	-	$^{VIII}Fe^{2+}$	$^5A \rightarrow {}^3B_3{}^{\oplus}$, $^5A \rightarrow {}^3B_1{}^{\oplus}$	$^5A_1 \rightarrow {}^3A_1$ (G), $^3B_3$ (H)
??	~25717	-	-	-	$^{VIII}Fe^{2+}$	results by fitting[TW]	
r	~27100-27225	27174	27125	27200[#]	$^{VI}Fe^{3+}$ ($^{VIII}Fe^{2+}$/Fe^{3+})[#/]	$^6A_{1g} \rightarrow {}^4E_g$ (^4D)[§, TW]	-
s	~28000[®]	-	~27970	-	Fe^{3+} ($^{VIII}Fe^{2+}$)$^{\oplus}$	$^5A \rightarrow {}^3B_3{}^{\oplus}$, $^5A \rightarrow {}^3B_1{}^{\oplus}$	-
t	~29000[⊕]/29100[¶]		~29350	-	$^{VIII}Fe^{2+}$	$^5A \rightarrow {}^3B_2{}^{\oplus}$, $^5A \rightarrow {}^3B_3{}^{\oplus}$, $^5A \rightarrow {}^3B_1{}^{\oplus}$	-
u	~29674[¥]/29762[†]	-	~30300	-	$^{VIII}Fe^{2+}$	-	-

690 Taran et al. (2007)[$], Khomenko et al. (2002)[®], Manning (1967)[⊕], Krambrock et al. (2013)[¶], Sangsawong et al. (2016)[¥], Sripoonjan et al. (2016)[†].

This is the peer-reviewed, final accepted version for American Mineralogist, published by the Mineralogical Society of America.
The published version is subject to change. Cite as Authors (Year) Title. American Mineralogist, in press.
DOI: https://doi.org/10.2138/am-2022-8500. http://www.minsocam.org/

691
692
693
694
695
696 Table 2. Spin-forbidden Mn^{2+} bands and their wavenumbers reported for various spessartine-rich garnets (left). They include a natural spessartine of
697 Moore and White (1972) together with their band labels[§], synthetic end-member spessartine of Smith and Langer (1983)[#], and several garnets with
698 spessartine mole fractions between 90 and 95 % of Laurs and Knox (2001)[†]. Those for nearly end-member spessartine GRR 43 at 293 and 78 K as
699 measured at CIT (middle - the given wavenumbers are not quantitative, because of the digitalization of the experimental spectrum recorded on chart
700 paper). Three spessartines measured in this work in Kyiv (right).

Sp70 (Table 5)[§]	Sp70 (Fig. 8)[§]	Sp100[#]	Sp90/95[†]	GRR 43 (293 K) Sp97	GRR 43 (78 K) Sp97	S-18 Sp93	271209132917 Sp91	GRR 2956 Sp84
-	-	19000	-	18960	18900	18940	18960	18990
-	-	-	-	-	19780 (Band h - Fe^{2+})	-	-	19800 (Band h - Fe^{2+})
20661 (j)	20661	20800	20704	20780	20680	20670	20710	20690
-	-	21600	21739	21740	21610	21690	21630	21660
-	23321?	23200	23256	23300	23190	23200	23190	23200
-	-	-	-	23300	23610	23670	23650	23670
23703 (n)	23702	23750	23753	23740	23880 23600	-	-	-
24200 (o)	24272	24300	-	24430	24340	24360	24360	24360
24516 (p)	24459	24500	24450	24580	24520	24450	24450	24450

This is the peer-reviewed, final accepted version for American Mineralogist, published by the Mineralogical Society of America.
The published version is subject to change. Cite as Authors (Year) Title. American Mineralogist, in press.
DOI: https://doi.org/10.2138/am-2022-8500. http://www.minsocam.org/

	26680	26680	
		27480	
		27940	
		28450	
		28940	

701

702

703

704

This is the peer-reviewed, final accepted version for American Mineralogist, published by the Mineralogical Society of America.
The published version is subject to change. Cite as Authors (Year) Title. American Mineralogist, in press.
DOI: https://doi.org/10.2138/am-2022-8500. http://www.minsocam.org/

Supplementary Table 3. Results of the curve-fitting analyses of the spin-forbidden bands for the spectra of two garnets with different almandine contents (Fig. 1a and b, respectively). Letter designations of the bands follow Moore and White (1972) and as modified in this study. Bands j*, "m′" and "??" are discussed in the text and noted in Fig. 1. FWHM is full width at half maximum. Compare to Table 1.

Band	Turtle Lake 17405762 – 23 Mol % Alm			Lind 3 – 69 Mol % Alm		
	Intensity (cm^{-1})	Energy (cm^{-1})	FWHM (cm^{-1})	Intensity (cm^{-1})	Energy (cm^{-1})	FWHM (cm^{-1})
d	0.384	14393	1911	1.292	14363	1789
e	0.423	16184	995	1.566	16210	1068
f	1.000	17388	1095	3.328	17361	1009
g	1.295	19162	1671	4.332	19120	1838
h	0.393	19812	355	1.250	19761	353
i	0.495	20144	621	1.859	20118	653
j*	0.459	20827	1114	1.232	20796	800
k	0.513	21839	1191	1.847	21656	1172
l	0.450	22892	935	1.232	22742	914
m	0.521	23566	806	2.036	23568	1095
m′	0.436	24217	886	0.477	24262	525
q	0.570	25122	1231	1.046	24847	901
"??"	0.400	26340	1219	1.094	25718	2243
r	0.442	27267	963	1.115	27097	973

Band "??" can possibly be assigned to a $^{6}A_{1g} \rightarrow {}^{4}T_{1g}$ (^{4}D) transition of $^{VI}Fe^{3+}$ (Table 1).

Figure Legends

Figure 1. Optical absorption spectra of two garnets as given by a black dotted line. a.) pyrope with 23 mol % almandine component (Turtle Lake - 17405762) and b.) almandine with 69 mol % almandine component (Lind 3). Both samples were measured in Kiev. The red line gives the fitted spectrum arising from the various underlying component bands. The band labels follow Moore and White (1972) with a few exceptions. We assign band j* to Fe^{2+} and not Mn^{2+} as these workers (see Table 1). There is a weak absorption feature that we label as band m'. The deconvolution analysis gives the band labelled "??". It does not have any clear expression in experimental spectra, but is needed to obtain reasonable fits to them. Supplementary Table 3 gives details on the spectral deconvolution and see the text for a full discussion.

Figure 2. Optical absorption spectra of nearly end-member spessartine GRR 43 (Sp97Alm3) at room (293 K) and liquid nitrogen (78 K) temperatures. They were measured at CIT on a Cary spectrometer using chart paper and the spectra were then scanned and digitalized. The arrows mark the positions of various possible spin-forbidden bands and the letters are the designations of Moore and White (1972).

Figure 3. Optical absorption spectra of five spessartines with different $Mn^{2+}/(Mn^{2+} + Fe^{2+})$ ratios. All crystals were measured in Kiev. Note: sample MMUR 32999/912 is an unusual F-bearing crystal (see Boiocchi et al. 2012) and sample Lind 2 is a pyrope-bearing spessartine (compositions given in Part I of this study). The letters correspond to those given by Moore and White (1972). Band n' is our designation. This absorption peak was assigned by the latter workers to $^{IV}Fe^{3+}$ (their band m).

Figure 4. Tanabe-Sugano diagram of a transition metal ion of electronic d^6 configuration (e.g., Fe^{2+}) taking B = 1080 cm^{-1} and C/B = 4.5 in a crystal field of cubic symmetry (plotted using the Excel file data at http://wwwchem.uwimona.edu.jm/). The vertical dash line indicates an approximate 10*Dq* value for $^{VIII}Fe^{2+}$ in garnet. The two levels, ^5E_g and $^5T_{2g}$, are shown by bold lines, because they have maximum quintet spin-multiplicity and they originate from the quintet ^5D term of a free ion (Dq = 0).

Figure 5. Tanabe-Sugano diagram of a transition metal ion of electronic d^5 configuration (e.g., Fe^{3+}, Mn^{2+}) taking B = 859 cm^{-1} and C/B = 4.5 in a crystal field of cubic symmetry (plotted using the Excel file data at http://wwwchem.uwimona.edu.jm/). The vertical dash line defines the 10*Dq* value and the solid circles show energies for the different sixtet-quartet spin-forbidden transitions. Only the sharp narrow bands arising from the crystal-field independent $^6A_{2g} \rightarrow {}^4A_{1g}$, ^4E_g (^4G) and $\rightarrow {}^4E_g$ (^4D) transitions of $^{VI}Fe^{3+}$ are observed in the spectra of almandine-pyrope garnets, that is, l, m and r, respectively (Fig. 1). Broader and weaker bands arising from the $^6A_{2g} \rightarrow {}^4T_{1g}$ (^4G) and $^6A_{2g} \rightarrow {}^4T_{2g}$ (^4G) transitions are obscured by more intense spin-forbidden bands of $^{VIII}Fe^{2+}$.

This is the peer-reviewed, final accepted version for American Mineralogist, published by the Mineralogical Society of America.
The published version is subject to change. Cite as Authors (Year) Title. American Mineralogist, in press.
DOI: https://doi.org/10.2138/am-2022-8500. http://www.minsocam.org/

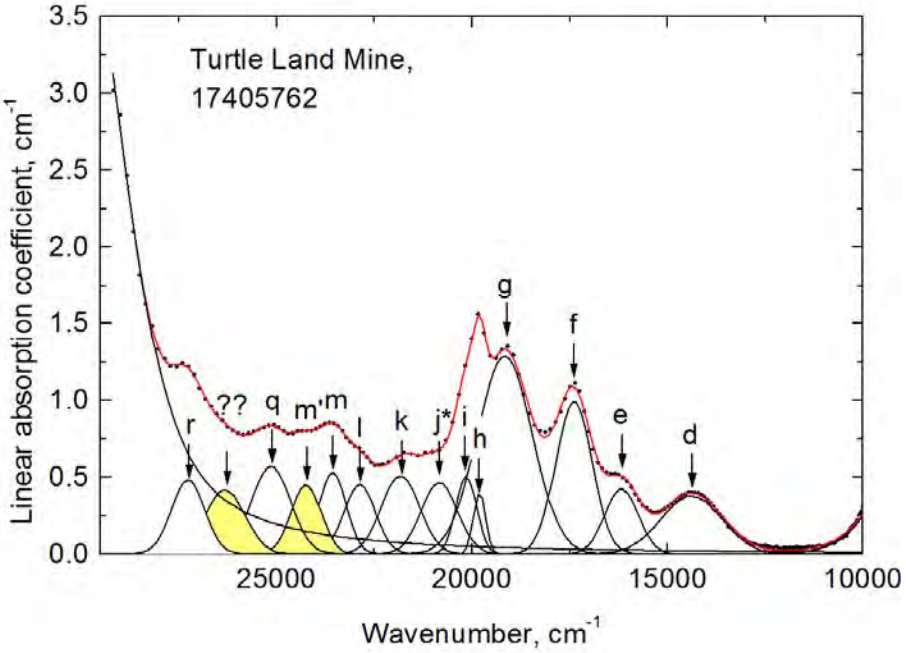

791

792 a)

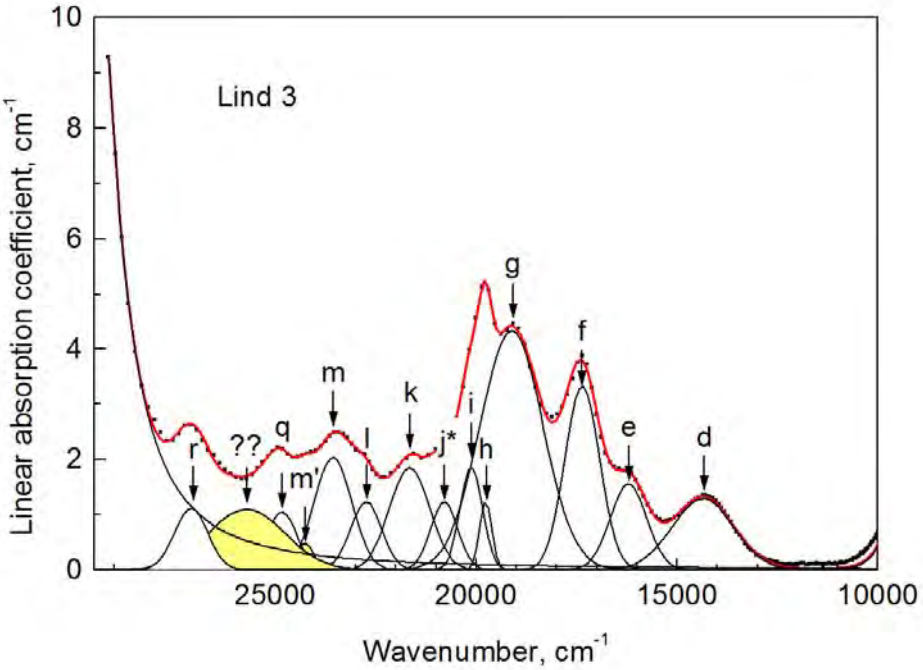

793
794 b)
795
796 Fig. 1.

This is the peer-reviewed, final accepted version for American Mineralogist, published by the Mineralogical Society of America.
The published version is subject to change. Cite as Authors (Year) Title. American Mineralogist, in press.
DOI: https://doi.org/10.2138/am-2022-8500. http://www.minsocam.org/

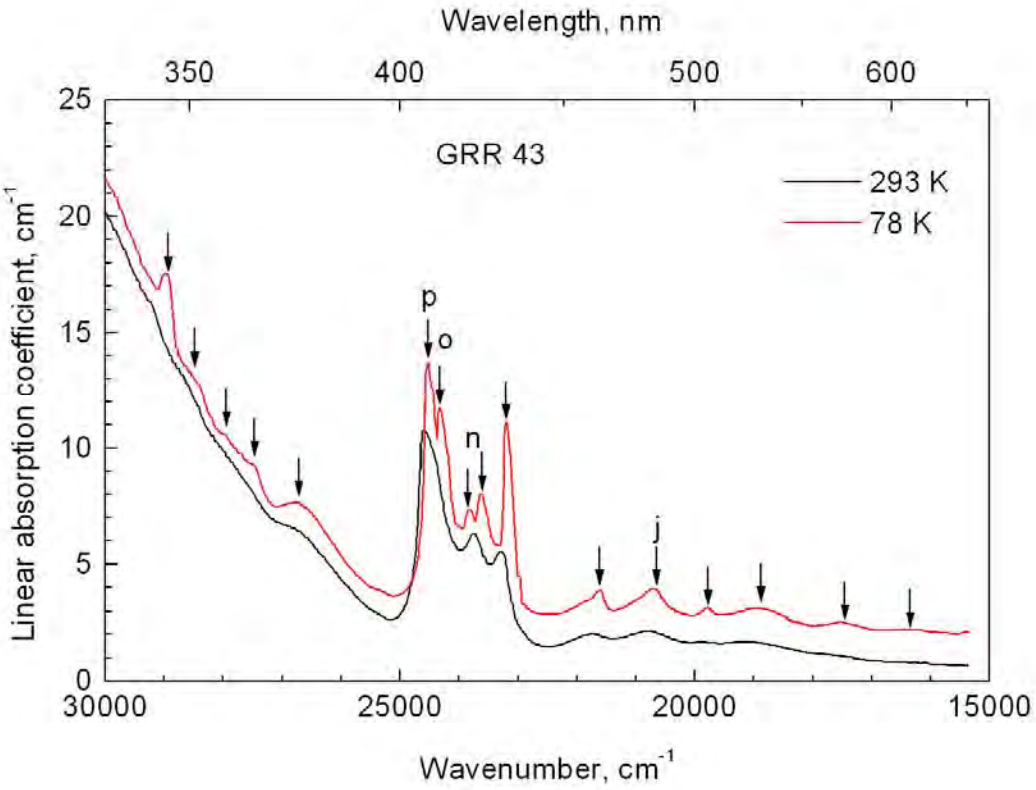

Figure 2.

This is the peer-reviewed, final accepted version for American Mineralogist, published by the Mineralogical Society of America.
The published version is subject to change. Cite as Authors (Year) Title. American Mineralogist, in press.
DOI: https://doi.org/10.2138/am-2022-8500. http://www.minsocam.org/

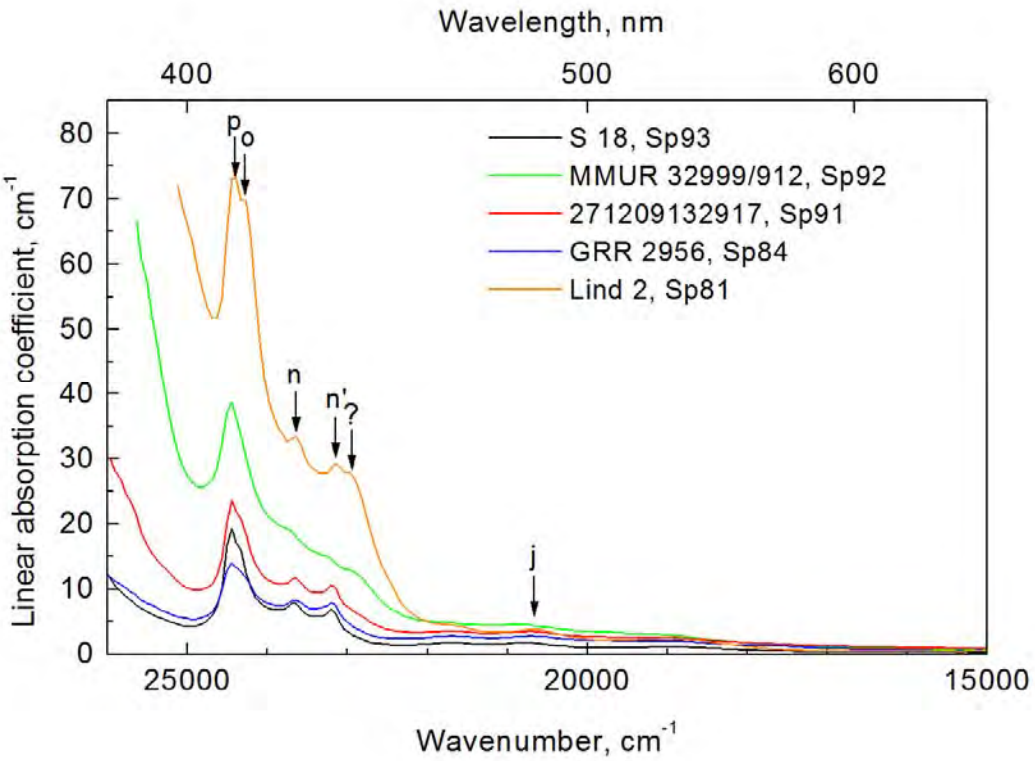

Figure 3.

This is the peer-reviewed, final accepted version for American Mineralogist, published by the Mineralogical Society of America.
The published version is subject to change. Cite as Authors (Year) Title. American Mineralogist, in press.
DOI: https://doi.org/10.2138/am-2022-8500. http://www.minsocam.org/

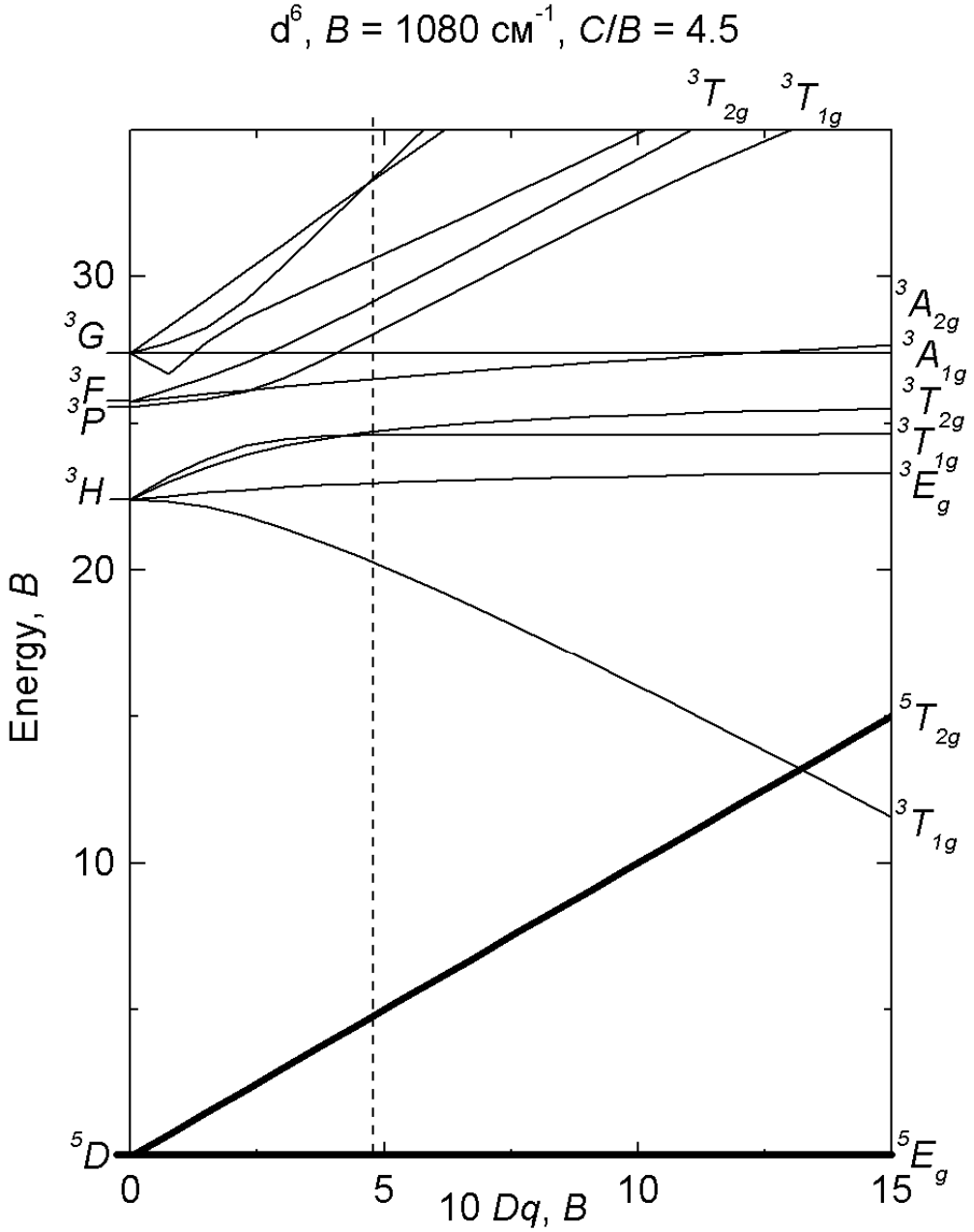

821

822

823 Figure 4.

824

825

This is the peer-reviewed, final accepted version for American Mineralogist, published by the Mineralogical Society of America.
The published version is subject to change. Cite as Authors (Year) Title. American Mineralogist, in press.
DOI: https://doi.org/10.2138/am-2022-8500. http://www.minsocam.org/

826

827

828

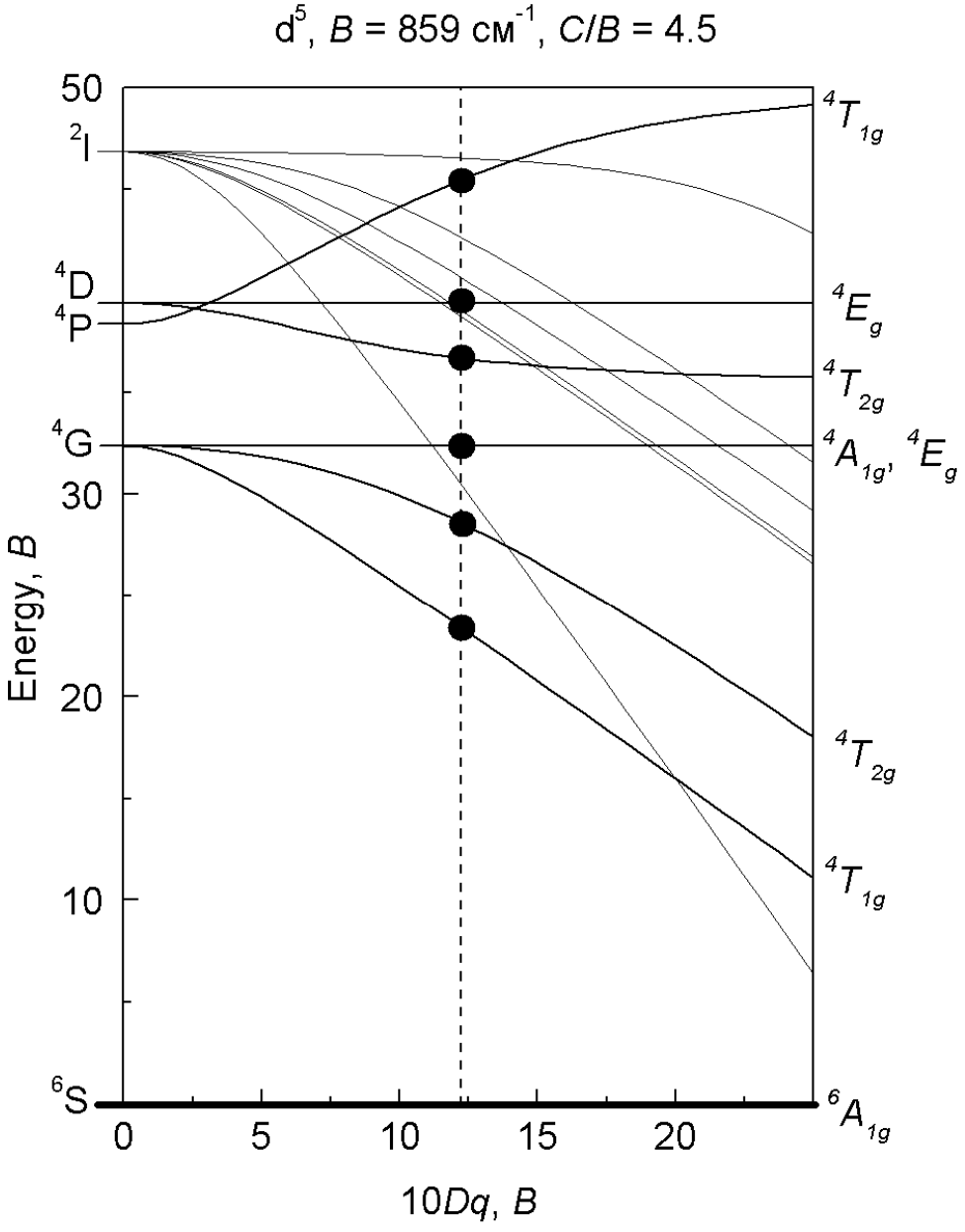

829

830

831 Figure 5.

832